Journal of Operation and Automation in Power Engineering

Vol. XX, No. XX, XXXX, Pages: XXXX (Proofed)

http://joape.uma.ac.ir

Research Paper

Distributionally Robust Chance-Constrained Energy Management of Microgrids Using Quantum Teaching Learning Based Optimization

Zahra Esmaeili [1], *Seyed Hamid Hosseini* [1, 2 *], and *Ali Ghaneian Sebdani* [1]

[1]*Department of Electrical Engineering, Sharif University of Technology, Tehran, Iran.*
[2]*Centre of Excellence in Power System Management and Control, Department of Electrical Engineering, Sharif University of Technology, Tehran, Iran.*

Abstract— *Optimal microgrid (MG) energy management is a critical issue due to the significant expansion of renewable energy sources (RESs). However, unpredictable changes in demand and the inherent intermittency of RESs lead to considerable uncertainties. In this paper, the distributionally robust chance-constrained (DRCC) method is combined with the quantum version of the teaching–learning-based optimization (quantum TLBO) algorithm for the first time to address the energy management problem of a grid-connected MG. Specifically, the DRCC method is employed to model uncertainties in both loads and RESs. Then, the quantum TLBO (QTLBO) algorithm is utilized to solve the energy management problem with the objective of minimizing the operating cost of the MG. The simulation results clearly demonstrate that the QTLBO algorithm outperforms the TLBO, differential evolution (DE), and real-coded genetic algorithm (RCGA) in terms of both convergence speed to the final optimal solution and the quality of the solution achieved. Additionally, the effectiveness of the proposed DRCC method in handling uncertainties is compared with the robust optimization (RO) method. Numerical simulation results show that the DRCC method combined with QTLBO is 23.58% more effective than the RO method combined with QTLBO.*

Keywords—Distributionally robust chance constrained, microgrid, optimal energy management, quantum teaching-learning-based optimization.

1. Introduction

With the advancement of technology and the resulting rise in global demand for power generation, microgrids (MGs) are emerging as a sustainable and practical solution. MGs are flexible and efficient energy systems operating at low or medium voltage [1]. Benefits of adopting MGs include enhanced voltage profiles, reduced greenhouse gas emissions, decentralized power supply, and decreased line losses. Additionally, consumers can actively participate in MG operations [2]. An MG can operate in either isolated or grid-connected mode. In grid-connected mode, it links to the grid via a Point of Common Coupling (PCC), enabling power exchange between the main grid and the MG. In remote areas where connection to the main grid is unfeasible due to technical or economic reasons, isolated MGs are implemented [1].

Energy management of an MG is a multi-objective, complex control system addressing various aspects, including technical domains, time scales, and physical levels. Therefore, a hierarchical control scheme is employed for efficient MG management. This scheme consists of three levels. The primary layer's main task is to locally and exclusively control the performance of each MG device, such as V/f, P/Q, and P/V. Power quality control, power distribution, and frequency coordination are managed in the secondary layer. Optimal energy management—including economic dispatch, load forecasting, and resource optimization at the distribution network level—is conducted in the third layer of the hierarchical control structure [3]. The present work focuses on MG energy management, situated at the third level of the MG hierarchical control structure.

The development of an Energy Management System (EMS) focuses on the optimal coordination of energy generation, consumption, and storage resources, considering both economic and technical aspects [4]. EMS ensures safety, stability, and efficiency for the MG [1]. However, integrating renewable energy sources (RESs) presents challenges in MGs due to their intermittent nature, complicating optimal energy management. If power variations are not accurately anticipated, costly reserves or ancillary services will be required, making MG operation uneconomical [2]. Additionally, inaccurate demand forecasting increases the complexity and uncertainty of scheduling and energy management in MGs [5, 6]. Thus, modeling uncertainties in this context is essential. To date, various mathematical methods, such as Information Gap Decision Theory (IGDT) [7–9], stochastic programming [10, 11], Robust Optimization (RO) [12], Chance-Constrained Programming (CCP) [13], and fuzzy techniques [14, 15], have been employed to address uncertainties in load, energy markets, and RESs output.

For instance, reference [16] employs a stochastic programming approach to address uncertainty in the output of RESs within a grid-connected MG. However, this method involves a significant computational burden and complexity. To mitigate these drawbacks, scenario reduction techniques have been applied in [16]. Since some scenarios are excluded from the solution process in scenario reduction methods, not all instances of uncertain parameter occurrences are considered when solving the problem [5]. In [17], a CCP-based formulation for the energy management problem

Received: 12 Apr. 2025
Revised: 02 Sept. 2025
Accepted: 27 Sept. 2025
*Corresponding author:
E-mail: hosseini@sharif.edu (S.H. Hosseini)
DOI: 10.22098/joape.2025.17159.2342

in MGs is proposed, considering uncertainties related to PV generation associated with solar radiation. Nonetheless, the two main drawbacks of the CCP technique are its high computational burden and its limitations in modeling all uncertain parameters with diverse characteristics [5]. In [18], an IGDT-based energy management system is presented for local energy communities, incorporating phase-change thermal energy storage. In [19], the RO method is employed to manage the uncertainty in loads and the power output of RESs, providing a robust scheduling solution. However, both the RO approach and the IGDT method are not well-suited for modeling random wind speed behaviors with significant ramping throughout the day, as they consider only worst-case scenarios for uncertain parameters [5]. Additionally, the results produced by the RO method tend to be conservative. To address the conservatism inherent in the RO method, Distributionally Robust Optimization (DRO) was proposed [6]. Unlike RO and stochastic programming methods, DRO does not require assumptions about specific distributions of uncertainties. In DRO, uncertainty is characterized by a set of ambiguities encompassing a range of distributions sharing similar statistics, such as instantaneous data [6]. Generally, DRO methods offer advantages that make them well-suited for application in power systems to manage renewable generation uncertainties for a MG [19], optimize bidding strategies in the electricity market, tackle power flow challenges [20], and enhance risk management amid increasing renewable energy penetration, among others. In [21], a DRO-based model is introduced to facilitate energy management of AC-DC hybrid MGs. The DRCC approach in [22] is employed to model uncertainties in renewable power generation and demand for transmission expansion planning. Unlike stochastic optimization, DRCC optimization makes fewer assumptions regarding the precise probability density functions (PDFs) of uncertainties and utilizes certain statistical properties, such as distribution moments or bounded deviations from a reference distribution. Compared to RO, DRCC optimization reduces conservatism by leveraging data within the ambiguity set and demonstrates more statistically optimal performance [23].

Based on the literature review, this paper considers the DRCC technique to model uncertainties in demand and RESs. The main requirement of MG EMS is to optimize MG operating costs. Various optimization methods have been proposed to address this issue, which can be categorized into two groups: (1) Mathematical optimization and (2) heuristic and meta-heuristic optimization. Unlike mathematical programming [24], classical metaheuristic algorithms can tackle non-differentiable and multidimensional problems; however, they do not guarantee achieving the global optimal solution [16].

Recently, research has focused on integrating quantum computing with classical optimization algorithms, leading to increased interest in quantum-inspired algorithms [25] These algorithms represent individuals using quantum bits, which contributes to their uniqueness and ability to find superior solutions. Furthermore, quantum representation enhances solution robustness and population diversity [26] because, unlike binary bits (which have two states: 0 and 1), quantum bits can exist in three states ($|0\rangle$, $|1\rangle$, $\frac{|0\rangle+|1\rangle}{\sqrt{2}}$) [16]. However, to date, quantum algorithms have been applied very limitedly in the MG energy management area [16].

To clarify the contribution of this paper, related works to the topic are listed in Table 1. This paper addresses the optimal energy management of a low-voltage grid-connected MG. Uncertainties in load and RESs are modeled using the DRCC method. The objective function, representing the cost of operating the MG, is minimized through the Quantum Teaching Learning Based Optimization (QTLBO) algorithm. The performance of QTLBO is compared with that of Teaching Learning Based Optimization (TLBO), Differential Evolution (DE), and Real-Coded Genetic Algorithm (RCGA). Additionally, the performance of the DRCC method is compared with the RO method.

The primary contributions of this paper are:

1) The DRCC method is integrated with the QTLBO algorithm for the first time to address the energy management issue of a low-voltage MG. Specifically, the DRCC method models uncertainties in both loads and RESs, followed by the application of the QTLBO algorithm to solve the energy management problem.
2) The results of the proposed method are compared with those of the RO method combined with QTLBO.
3) A graph illustrating the QTLBO algorithm's results based on the number of runs is presented, demonstrating the effectiveness of the QTLBO algorithm.
4) The superiority of QTLBO over its non-quantum counterpart, TLBO, as well as over the DE method and RCGA, is established.

The remainder of this paper is structured as follows: Section 2 addresses MG modeling and presents the problem formulation, DRCC model, and problem constraints. Section 3 describes the QTLBO algorithm. Finally, simulation results, conclusions, and recommendations for future work are provided in Sections 4 and 5, respectively.

2. STUDIED SYSTEM AND RELATED MATHEMATICAL EQUATIONS

A typical low-voltage MG comprising components such as WT, Photovoltaic (PV) system, Fuel Cell (FC), Microturbine (MT), and Battery Energy Storage System (BESS) is examined in this paper. As illustrated in Fig. 1, this MG is grid-connected, with energy exchange managed by a Microgrid Central Controller (MGCC).

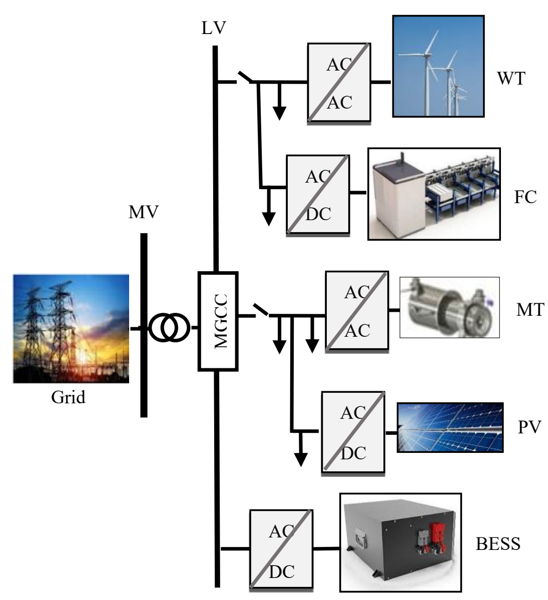

Fig. 1. A typical low voltage MG.

2.1. Problem fotmulation

In this paper, the output power of resources and battery consumption are optimized to achieve the lowest operating cost. The objective function is expressed in Eq. (1). The symbol X denotes the optimal values of the decision variables, which are $P^t_{DG_y}$, $P^t_{BESS_z}$, and P^t_{grid}.

Table 1. Summary of literature review.

Ref.	Uncertainty modeling	Optimization technique	Uncertainty in load	Uncertainty in RESs
[5]	DRCC	MINLP	✓	✓
[6]	DRCC	Stochastic optimization	✓	✓
[16]	Stochastic optimization	QTLBO	–	✓
[27]	DRCC	Stochastic optimization	✓	✓
[21]	DRO	MILP	✓	✓
This work	**DRCC**	**QTLBO**	✓	✓

$$Min\,f(X) = \sum_{t=1}^{T} Operation\,\mathrm{Cost}^t = \sum_{t=1}^{T} OC^t = \sum_{t=1}^{T}\left\{\sum_{y=1}^{NG}\left[u_y^t P_{DG_y}^t B_{DG_y}^t + S_{DG_y}\left|u_y^t - u_y^{t-1}\right|\right] + \sum_{z=1}^{NS}\left[v_z^t P_{BESS_z}^t B_{BESS_z}^t + S_{BESS_z}\left|v_z^t - v_z^{t-1}\right|\right] + P_{grid}^t B_{grid}^t\right\} \quad (1)$$

where t (hours) denotes time, and $T = 24$. v_z^t and u_y^t illustrate the on/off modes of the z^{th} BESS and the y^{th} Distributed Generation (DG) at time t, respectively. $B_{BESS_z}^t$ and $B_{DG_y}^t$ indicate the costs of turning on/off the z^{th} BESS and the y^{th} DG, respectively. and represent the bid prices of the z^{th} BESS and the y^{th} DG at time t, for output powers $P_{BESS_z}^t$ and $P_{DG_y}^t$, respectively. NS and NG show the number of BESS units and DG units, respectively. B_{grid}^t shows the main grid market price for power P_{grid}^t at time t. PV, WT, MT, and FC units are considered DGs.

The constraints of the MG energy management problem are outlined as follows:

A) Power balance constraint

According to Eq. (2), the power generated each hour must equal the load for that hour.

$$\sum_{l=1}^{ND} P_{Demand_l}^t = \sum_{y=1}^{NG} P_{DG_y}^t + \sum_{z=1}^{NS} P_{BESS_z}^t + P_{grid}^t; \forall t \in 1,2,...,T \quad (2)$$

where ND displays the number of loads.

B) WT power constraint

According to Eq. (3), the WT output power must not exceed its maximum allowable value.

$$0 \le P_{WT}^t \le P_{WT,UP}^t \qquad \forall t \in 1,2,...,T \quad (3)$$

where $P_{WT,UP}^t$ represents the upper limit of WT power.

C) PV power constraint

PV power constraints are defined in accordance with Eq. (4).

$$0 \le P_{PV}^t \le SOL^t.S_{PV}.\eta_{PV} \qquad \forall t \in 1,2,...,T \quad (4)$$

where SOL^t represents the solar radiation at time t, S_{PV}, and η_{PV} denote the PV panel size and the efficiency of the PV system, respectively. The uncertainty in the PV unit output arises from the variability of solar radiation.

D) Minimum and maximum output power limits

The minimum and maximum output power limits of DG units, the main grid, and BESS are specified in Eq. (5).

$$\begin{cases} P_{DG_y,\min}^t \le P_{DG_y}^t \le P_{DG_y,\max}^t \\ P_{grid,\min}^t \le P_{grid}^t \le P_{grid,\max}^t \\ P_{BESS_z,\min}^t \le P_{BESS_z}^t \le P_{BESS_z,\max}^t \end{cases} \quad (5)$$

where, $P_{DG_y,\min}^t$ and $P_{DG_y,\max}^t$ are the minimum and maximum output powers of the y^{th} DG unit at time t, respectively. $P_{grid,\min}^t$ and $P_{grid,\max}^t$ indicate the minimum and maximum output powers of the main grid at time t, respectively. $P_{grid,\min}^t$ and $P_{grid,\max}^t$ denote the minimum and maximum stored/consumed powers of the z^{th} BESS at time t, respectively.

E) MT ramping constraint

The MT ramping constraint is specified in Eq. (6).

$$-DR_{MT} \le P_{MT}^t - P_{MT}^{t-1} \le UR_{MT} \quad (6)$$

where, DR_{MT} represents the minimum ramp rate of the MT. UR_{MT} indicates the maximum ramp rate of the MT. P_{MT}^t and P_{MT}^{t-1} denote the MT output power at time t and time $t-1$, respectively.

F) Main grid constraint

Eq. (7) defines the acceptable range for the output power of the main grid. To prevent infeasible solutions (outside the acceptable range), a quadratic expression as given in Eq. (8) is incorporated into the objective function.

$$P_{grid,l}^t = \begin{cases} P_{grid,\max}^t & \text{if } P_{grid}^t \succ P_{grid,\max}^t \\ P_{grid,\min}^t & \text{if } P_{grid}^t \prec P_{grid,\min}^t \\ P_{grid}^t & \text{if } P_{grid,\min}^t \le P_{grid}^t \le P_{grid,\max}^t \end{cases} \quad (7)$$

$$f(X) = \sum_{t=1}^{T} OC^t + \lambda_{pen}\left(P_{grid}^t - P_{grid,l}^t\right)^2 \quad (8)$$

where, λ_{pen} represents the penalty factor.

G) Demand constraint

As shown in Eq. (9), the load demand can vary between a minimum and a maximum value each hour.

$$P_{Demand,Down}^t \le P_{Demand}^t \le P_{Demand,UP}^t \qquad \forall t \in 1,2,...,T \quad (9)$$

where, $P_{Demand,Down}^t$ and $P_{Demand,UP}^t$ are the lower and upper limits of demand at time t.

2.2. DRCC model

The DRCC method is a technique for addressing uncertainties. It combines two approaches: DRO [21] and CCP [28].

The fluctuating behavior of uncertain parameters makes related constraints probabilistic. The DRCC method is a powerful tool that effectively models probability-based constraint problems. Furthermore, it is used to minimize MG operation costs or to maximize MG profits with a specified probability, based on the system's robustness [5]. The complete proof of the DRCC mathematical equations is provided in [5].

2.3. DRCC model applied to problem formulation

When applying the DRCC method to the problem of optimal MG management, several constraints outlined in Subsection 2.1 are modified. The constraints that are altered are as follows:

A) WT power constraint

$$0 \le P_{WT}^t \le P_{WT,UP}^t - \left(\sqrt{\frac{\varpi}{1-\varpi}}\right) \times \left(\sigma_{P_{WT,UP}^t}\right) \tag{10}$$

where, $P_{WT,UP}^t$ is the upper limit of WT power. $\sigma_{P_{WT,UP}^t}$ and ϖ denote the standard deviation and confidence level of WT power, respectively.

B) PV system power constraint

$$0 \le P_{PV}^t \le (S_{PV}.\eta_{PV}).\left(SOL^t - \left(\sqrt{\frac{v}{1-v}}\right) \times (\sigma_{SOL^t})\right) \tag{11}$$

where, v is the PV system confidence level. S_{PV} and η_{PV} are the size of the PV panel and the efficiency of the PV system, respectively. SOL^t is the solar radiation at time t. σ_{SOL^t} is the standard deviation of solar radiation at time t.

C) Demand constraint

$$P_{Demand}^t \le P_{Demand,UP}^t - \left(\sqrt{\frac{\varpi_D}{1-\varpi_D}}\right) \times \left(\sigma_{P_{Demand,UP}^t}\right) \tag{12}$$

$$P_{Demand}^t \ge P_{Demand,Down}^t - \left(\sqrt{\frac{\varpi_D}{1-\varpi_D}}\right) \times \left(\sigma_{P_{Demand,Down}^t}\right) \tag{13}$$

where $P_{Demand,UP}^t$, $P_{Demand,Down}^t$, and ϖ_D are the upper limit, lower limit, and confidence level of demand, respectively. $\sigma_{P_{Demand,UP}^t}$ and $\sigma_{P_{Demand,UP}^t}$ are the standard deviations of demand.

3. REVIEW OF OPTIMIZATION METHODS

3.1. Review of TLBO

The TLBO algorithm is inspired by the teaching-learning process in a classroom and was first introduced by Rao *et al.* in 2011. Its easy implementation, lack of algorithm-specific parameters, straightforward concept, rapid convergence, and effectiveness are among the features that have attracted researchers' attention. Unlike swarm intelligence and traditional evolutionary algorithms, the repetitive computation process of TLBO is divided into two stages, each involving a repetitive learning operation [29]. The first stage is called the teacher phase, while the second is the learner phase. In the first stage, the teacher aims to improve the class's average grade. In the second stage, students interact with one another to enhance their knowledge [16]. The student with the best fitness value from the initial population is chosen as the teacher, represented by the symbol X_{best}. At this point, the new solution is determined according to Eq. (14) [29].

$$X_{i,new} = X_{i,old} + rand_k\left(X_{i,best} - T_F * X_{i,mean}\right) \tag{14}$$

$rand_k$ represents a random number in the k^{th} iteration, ranging from [0,1]. The teaching factor (T_F) is a fixed value randomly chosen to be either 1 or 2. During the learning phase, students enhance their knowledge through interactions. If student X_i has more knowledge than student X_j, the new solution is updated according to Eq. (15); otherwise, it is determined by Eq. (16) [29].

$$X_{i,new} = X_{i,old} + rand_k\left(X_i - X_j\right) \tag{15}$$

$$X_{i,new} = X_{i,old} + rand_k\left(X_j - X_i\right) \tag{16}$$

The integration of population-based evolutionary computations with quantum computations enhances the performance of traditional heuristic algorithms [16]. The theory of quantum computing is briefly discussed below, followed by a description of the QTLBO algorithm.

3.2. Introduction to quantum computation

Although population representation and fitness assessment are considered distinct in both quantum search algorithms and traditional intelligent algorithms, population elements in quantum search algorithms are represented as quantum bits (not binary). Quantum bits can exist in three states:

(1) state "1", (2) state "0", or (3) any superposition of both states. As illustrated in Fig. 2, enhancing population diversity is one advantage of quantum bit representation over binary representation [26]. A quantum bit string or quantum register containing m quantum bits is represented as $Q(k) = \left[q_1^k, q_2^k, ..., q_m^k\right]$, indicating that 2^m states exist simultaneously. The diversity of the initial population in the quantum register arises from the probabilistic superposition state [26].

A specific variation operator modifies the eigenstate of quantum bits. This operator is known as the quantum gate. Various quantum gates exist, including the Hadamard gate, NOT gate, phase shift gate, rotating gate, etc. [25]. According to quantum mechanics principles, a superposition state collapses to a single state upon observing a coherent state. The intrinsic characteristics of quantum gates cause each quantum bit to converge to a single eigenstate.

Furthermore, they enhance the solution by balancing exploitation and exploration. To modify individual quantum bits in a string, a quantum gate ($R(\theta_i)$) is used as shown in Eq. (17) [16].

$$\begin{gathered}\left|\begin{matrix}\alpha'_i \\ \beta'_i\end{matrix}\right| = R(\theta_i)\left|\begin{matrix}\alpha_i \\ \beta_i\end{matrix}\right| = \\ \begin{bmatrix}\cos(\theta_i) & -\sin(\theta_i) \\ \sin(\theta_i) & \cos(\theta_i)\end{bmatrix}\left|\begin{matrix}\alpha_i \\ \beta_i\end{matrix}\right|\end{gathered} \tag{17}$$

where θ_i represents the rotation angle. The purpose of the rotation angle is to control individual quantum bits as they converge to a single state.

(α'_i, β'_i) indicates the modified value of the (α'_i, β'_i) is derived from the quantum gate operator and achieves the final convergent state. Fig. 3 illustrates the polar diagram of the quantum bit rotation process.

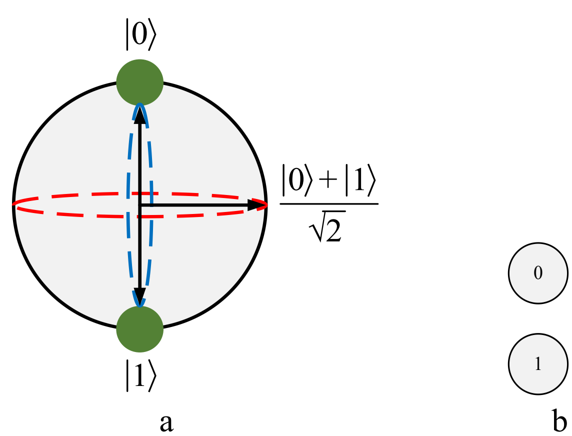

Fig. 2. (a) Display of quantum bit, (b) Display of binary bit.

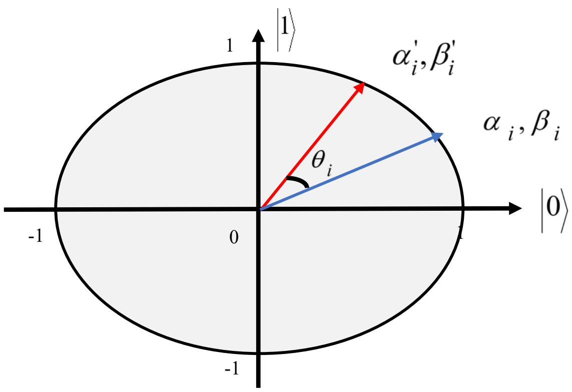

Fig. 3. The polar diagram demonstration of quantum bit rotating.

3.3. QTLBO algorithm

QTLBO is an enhanced optimization algorithm that utilizes the properties of quantum behavior particles, improving the performance of TLBO by addressing multiple local optima in the search space [30]. All QTLBO formulations, along with detailed descriptions, are provided in [16, 30]. These formulations are summarized as follows:

The quantum population in the QTLBO algorithm consists of P students, each studying M subjects in a course. The vector representing the i^{th} student at the k^{th} iteration is defined according to Eq. (18), where $i = 1, 2, ..., P$ and $m = 1, 2, . \; . \; . \; , M$.

$$X_i^k = \left(X_{i,1}^k, X_{i,2}^k, ..., X_{i,m}^k\right) = \left[\begin{array}{l} \alpha_{i,1}^k, \alpha_{i,2}^k, ..., \alpha_{i,m}^k \\ \beta_{i,1}^k, \beta_{i,2}^k, ..., \beta_{i,m}^k \end{array}\right] \tag{18}$$

where, $\alpha_{i,m}^k$ and $\beta_{i,m}^k$ denote the quantum states of the quantum bit individuals. To select a quantum teacher, the fitness value ($f\left(\bar{X}_i^k\right)$) of the quantum string is first determined.

Then, the learner with the best fitness is identified and selected as the quantum teacher. $\bar{X}_i^k$ indicates the mapping of X_i^k in Eq. (18).

In the quantum teaching phase, the quantum teacher's role is to enhance the progress of the learners in the class. Learners learn from the quantum teacher with a probability of p. During the iteration process, each learner calculates the value of the quantum teacher and their mean result, then updates the new solution according to Eq. (19), based on the difference between these two values.

$$D_{i,m}^{k+1} = r_{i,m}^k \left(X_b^k - TF_{i,m}^k \times X_{mean}^k\right) \tag{19}$$

where, $D_{i,m}^{k+1}$ represents the i^{th} student's difference for the m^{th} subject at the $(k+1)^{th}$ iteration. X_b^k and X_{mean}^k are the solutions of the quantum teacher and the mean value of the quantum learners at the k^{th} iteration, respectively. $r_{i,m}^k$ displays a random number in the range [0,1]. $TF_{i,m}^k$ is the teaching factor that controls the mean result of quantum learners. $TF_{i,m}^k = round\left(1 + rand\left(0,1\right)\right)$ can be either $1 \; or \; 2$. $rand \; (.)$ represents a random number in the range [0,1]. The i^{th} student can also learn from other quantum learners with a probability of $1-p$. This prevents the solution from becoming trapped in a local optimum. Hence, Eq. (19) is modified to Eq. (20).

$$D_{i,m}^{k+1} = r_{i,m}^k \left(X_b^k - X_{mean}^k\right) + LF_{i,m}^k \times \delta_{i,m}^k \left(X_{mean}^k - X_{i,m}^k\right) \tag{20}$$

where, $LF_{i,m}^k$ is a random number referred to as the learning factor. $\delta_{i,m}^k$ is known as the convergence coefficient, and its equation is presented in Eq. (21). The convergence coefficient enhances the global search capability of the algorithm.

$$\delta_{i,m}^k = 1 - 0.9 \times \frac{k}{k_{\max}} \tag{21}$$

$k_{\max}$ indicates the maximum number of iterations, which is set to 150 in this paper. In the teaching phase, the temporary quantum state (Q_i^{k+1}) is defined according to Eq. (22).

$$Q_{i,m}^{k+1} = \left|X_{i,m}^k \cos\left(D_{i,m}^{k+1}\right) \pm \sqrt{1-\left(X_{i,m}^k\right)^2} \sin\left(D_{i,m}^{k+1}\right)\right| \times \log\frac{1}{u} \tag{22}$$

u represents a random number within the range [0,1]. $rand \; (.)$ and u are designed to improve the exploitation features of QTLBO. If $rand \; (.)$ takes a value greater than 0.5, the negative term in Eq. (22) is applied based on the quantum behavior learning strategy; otherwise, the positive term is used.

Due to the interactions quantum learners have with one another during the quantum learning phase, their knowledge in each subject increases. If the i^{th} learner possesses a higher fitness level than the j^{th} learner, the i^{th} learner shares his/her knowledge with the latter.

The difference between these two learners is calculated according to Eq. (23).

$$D_{i,m}^{k+1} = \begin{cases} IF_{i,m}^k \left(Q_{i,m}^{k+1} - Q_{j,m}^{k+1}\right) & Q_i^{k+1} \succ Q_j^{k+1} \\ IF_{i,m}^k \left(Q_{j,m}^{k+1} - Q_{i,m}^{k+1}\right) & Q_i^{k+1} \prec Q_j^{k+1} \end{cases} \tag{23}$$

where, $D_{i,m}^{k+1}$ is the difference between the i^{th} and j^{th} quantum learners for the m^{th} subject. $IF_{i,m}^k$ is a random number selected as an interacting factor to regulate the interaction process. In the learning phase, the new solution is determined according to Eq. (24).

$$X_{i,m}^{k+1} = \left|Q_{i,m}^{k+1} \cos\left(D_{i,m}^{k+1}\right) \pm \sqrt{1-\left(Q_{i,m}^{k+1}\right)^2} \sin\left(D_{i,m}^{k+1}\right)\right| \times \log\frac{1}{u} \tag{24}$$

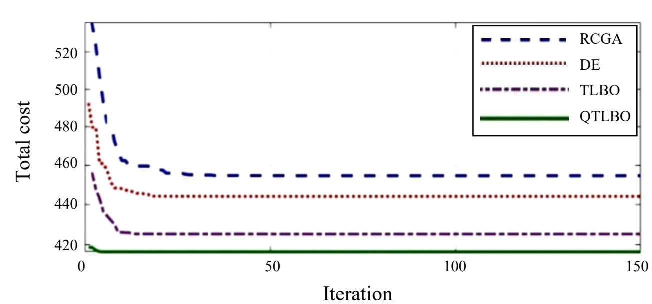

Fig. 4. The cost function curves acquired from the algorithms.

u, a random number within the range [0,1], is used to enhance the QTLBO exploitation features [30]. As stated in Eq. (22), if $rand \; (.)$ yields a value less than 0.5, the positive term in Eq.

Table 2. QTLBO pseudo-code.

Step	Description
1	**Begin**
2	Initialize population size (P) and number of decision variables (M)
3	Initialization of the quantum learners X_i^k and measurement of their fitness amounts
4	Put the best quantum learner as the teacher
5	**while** $k \prec k_{\max}$
6	**for** $i = 1, 2, \ldots, P\%$ quantum teaching phase
7	**for** $m = 1, 2, \ldots, M$
8	$TF_{i,m}^k = round\,(1 + rand\,(0, 1))$
9	Measure the difference between X_{mean} and X_b according Eq. (22)
10	Update the state of temporary quantum $Q_{i,m}^{k+1}$
11	**end for**
12	Select $Q_{i,m}^{k+1}$ if $f\left(\bar{Q}_{i,m}^{k+1}\right) \succ f\left(\bar{X}_{i,m}^{k}\right)$
13	**end for**
14	**for** $i = 1, 2, \ldots, P\%$ (quantum learning phase)
15	**for** $m = 1, 2, \ldots, M$
16	Choose a random partner j from the quantum learners
17	**if** $f\left(Q_i\right) \succ f\left(Q_j\right)$
18	measure $IF_{i,m}^k\left(Q_{i,m}^{k+1} - Q_{j,m}^{k+1}\right)$
19	**else**
20	measure $IF_{i,m}^k\left(Q_{j,m}^{k+1} - Q_{i,m}^{k+1}\right)$
21	**end if**
22	Update the solution $X_{i,m}^{k+1}$ and measure the fitness amount according to
23	**end for**
24	Select $X_{i,m}^{k+1}$ if $f\left(\bar{X}_i^{k+1}\right) \succ f\left(\bar{Q}_i^{k+1}\right)$ and update the quantum teacher
25	**end for**
26	**end while**
27	**end**

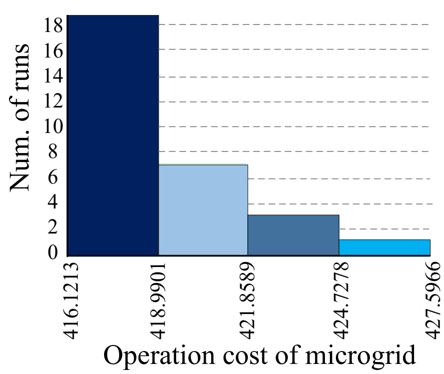

Fig. 5. Number of the QTLBO algorithm runs versus MG operation cost.

(24) is applied based on the quantum behavior learning strategy; otherwise, the negative term is used.

To determine the fitness $f\left(\bar{X}_i^{k+1}\right)$, the mapping $X_{i,m}^{k+1}$, referred to as the latent temporary solution, is evaluated. A greedy choice is employed to select the better between $X_{i,m}^{k+1}$ and $Q_{i,m}^{k+1}$. The fitness value dictates the optimal choice. Upon meeting the algorithm's termination criterion, the final solution $X_{i,m}^{k+1}$ is obtained. Table 2 presents the QTLBO pseudo-code.

4. SIMULATION RESULTS

Optimal energy management is evaluated on a grid-connected MG, whose structure is illustrated in Fig. 1, with additional details available in [16] and [31]. Predicted load data and market prices for the upcoming 24 hours are sourced from [16]. The DRCC method accounts for demand uncertainty and variations in RESs, with further information on the DRCC method provided in [5].

The optimization problem is solved using the QTLBO algorithm, and its results are compared with those from the TLBO, DE, and RCGA algorithms. For all algorithms mentioned, the population size is set to be 200, and the maximum number of iterations is 150. For the RCGA algorithm, the crossover and mutation distribution indices are set to 4, with crossover and mutation probabilities of 0.8 and 0.2, respectively. In the DE algorithm, the crossover probability is 0.7, and the scaling factor is 0.5.

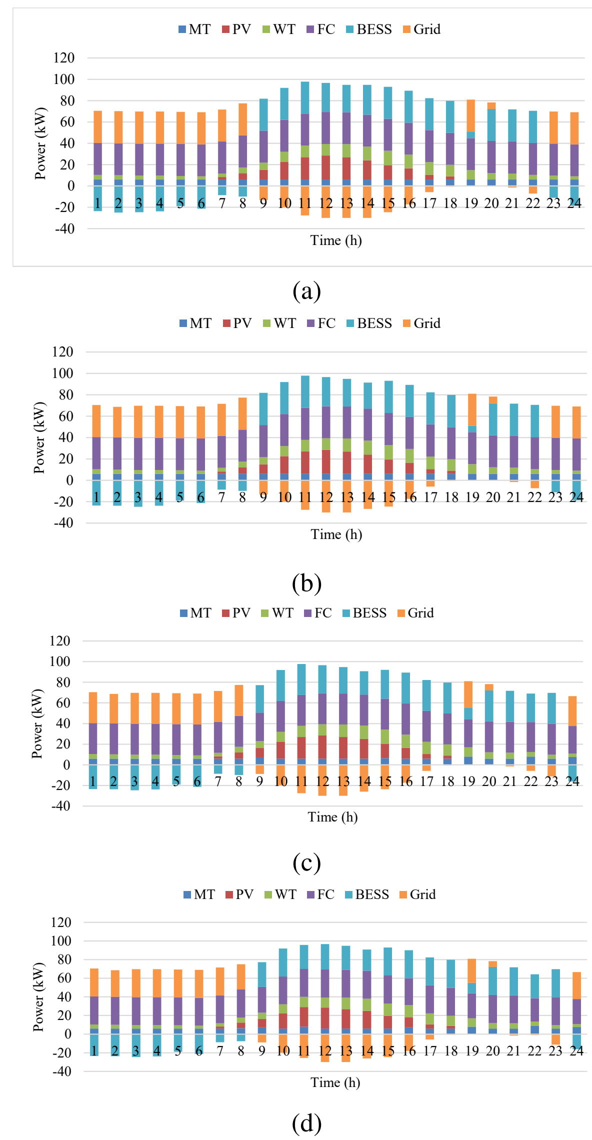

Fig. 6. Generation of MG's DERs: (a) Using QTLBO, (b) Using TLBO, (c) Using DE; (d) Using RCGA.

The optimization results from the QTLBO algorithm are presented in Tables 3 and 4. In these tables, positive and negative terms in the cost column indicate costs and benefits, respectively. In Table 3, the positive and negative symbols in the grid power column indicate purchasing power from the main grid and selling power back to it, respectively. In the BESS column, a negative sign indicates that BESS is charging, while a positive sign indicates discharging. As seen in Table 3, the highest PV power generation occurs during the hours when the sun is at its peak. Also, the highest WT power generation is achieved when the wind conditions are favorable (in terms of direction and speed). As shown in Table 3, grid power is negative during hours with high electricity prices (10 a.m., 11 a.m., 12 p.m., and 2 p.m.), while BESS power is positive. This indicates that, besides power generation sources, power is also drawn from the BESS during these hours to supply the microgrid loads and sell excess power to the grid, thereby generating profits. These findings demonstrate that QTLBO effectively optimizes the MG energy management problem.

The operation costs resulting from the QTLBO, TLBO, DE, and RCGA algorithms are 416.1213 €ct, 428.9162 €ct, 446.2825 €ct, and 453.2905 €ct, respectively, as illustrated in Fig. 4. Fig.

Table 3. The MG energy management results using the QTLBO algorithm.

Time (h)	P_{load} (kW)	P_{grid} (kW)	P_{BESS} (kW)	P_{FC} (kW)	P_{WT} (kW)	P_{PV} (kW)	P_{MT} (kW)	**Cost €ct**
1	46.8	30	-23.587	30	4.387	0	6	16.8162
2	45.0	30	-25.050	30	4.050	0	6	12.0887
3	45.0	30	-24.713	30	3.713	0	6	10.3551
4	45.9	30	-23.813	30	3.713	0	6	10.0971
5	50.4	30	-18.975	30	3.375	0	6	11.5729
6	47.7	30	-21.338	30	3.038	0	6	12.7133
7	63.0	30	-8.625	30	3.375	2.25	6	24.6199
8	67.5	30	-9.908	30	5.400	6.008	6	40.5158
9	68.4	-13.35	30.000	30	6.750	9.000	6	33.4358
10	72.0	-19.94	30.000	30	9.450	16.492	6	-4.0508
11	70.2	-27.59	30.000	30	10.80	20.992	6	-21.5743
12	66.6	-30.00	27.300	30	10.80	22.500	6	-28.3356
13	64.8	-30.00	25.725	30	12.15	20.925	6	43.4446
14	64.8	-30.00	27.975	30	12.83	18.000	6	-37.5343
15	68.4	-24.60	30.000	30	13.50	13.500	6	23.1315
16	72.0	-17.33	30.000	30	12.83	10.508	6	30.0765
17	76.5	-5.81	30.000	30	11.81	4.500	6	43.7752
18	79.2	-0.59	30.000	30	10.80	2.993	6	42.0412
19	81.0	30	6.225	30	8.775	0	6	33.8431
20	78.3	6.225	30.000	30	6.075	0	6	32.1572
21	70.2	-1.537	30.000	30	5.737	0	6	27.3195
22	63.2	-7.187	30.000	30	4.387	0	6	23.7883
23	58.5	30	-11.213	30	3.713	0	6	20.2851
24	50.4	30	-18.638	30	3.038	0	6	15.5393
Total Cost = 416.1213 €ct								

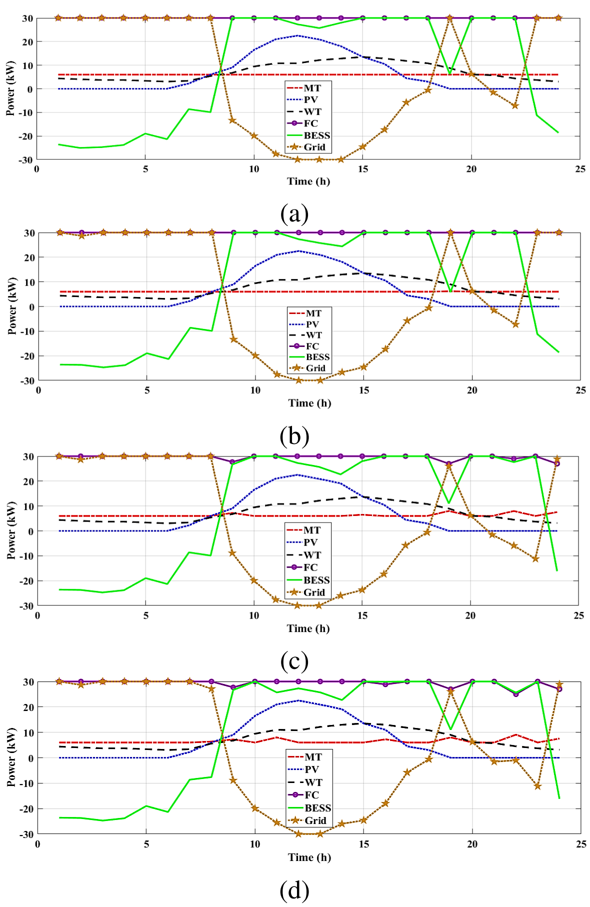

Fig. 7. MG resources' hourly powers: (a) Using QTLBO, (b) Using TLBO, (c) Using DE; (d) Using RCGA.

4 shows that the QTLBO algorithm converged to the final optimal value faster than the other algorithms and also achieved superior results.

Fig. 5 presents the outcomes of the QTLBO algorithm over multiple runs. Among 30 runs of the QTLBO algorithm, the best result is 416.1213 €ct, while the worst result is 427.5966 €ct, as shown in Fig. 5. Thus, there is only a 2.76% difference between the worst and best results of the QTLBO algorithm. Notably, the worst result from the 30 runs of the QTLBO algorithm is still better than the best results from the other algorithms.

The hourly generation of MG's DERs using the QTLBO, TLBO, DE, and RCGA algorithms is depicted in Fig. 6. The hourly power resources of the MG obtained through the QTLBO, TLBO, DE, and RCGA algorithms are shown in Fig. 7. These figures illustrate the power production and consumption of each source for every hour. As observed in Figs. 6 and 7, the power variation patterns of different sources are nearly identical across all four algorithms.

To verify the results, the outcome from the DRCC method is compared with that from the RO method. Table 5 demonstrates the MG operation costs derived from these two methods. As shown in Table 5, the result from the RO method exceeds that of the DRCC method. The result related to the DRCC method is 23.58% better than that of the RO method. This comparison validates the results, as the RO method is conservative, making such a result expected.

5. Conclusion

This paper addresses the optimal energy management of a grid-connected MG comprising RESs and non-RESs, BESS, and loads. RESs include WT and PV systems, while non-RESs consist of MT and FC. The uncertainties in loads, WT power, and PV power are considered. In this study, these uncertainties are modeled using the DRCC method. The quantum version of the TLBO algorithm is employed to solve the MG energy management problem. The optimization objective is to minimize the operational costs of the MG. Based on the results presented in this work, the QTLBO algorithm has effectively optimized the energy management problem of the MG so that, during peak

Table 4. The operation cost of each component of the microgrid (MG).

Time (h)	Grid (€ct)	BESS (€ct)	FC (€ct)	WT (€ct)	PV (€ct)	MT (€ct)	Total cost (€ct)
1	6.9	-8.9631	10.47	4.7072	0	3.702	16.8162
2	5.7	-9.5190	8.82	4.3456	0	2.742	12.0887
3	4.2	-9.3909	8.82	3.9840	0	2.742	10.3551
4	3.6	-9.0489	8.82	3.9840	0	2.742	10.0971
5	3.6	-7.2105	8.82	3.6214	0	2.742	11.5729
6	6.0	-8.1084	8.82	3.2598	0	2.742	12.7133
7	6.9	-3.2775	8.82	3.6214	5.8140	2.742	24.6199
8	11.4	-3.7650	8.82	5.7942	15.5247	2.742	40.5158
9	-20.025	11.4000	8.82	7.2428	23.2560	2.742	33.4358
10	-79.768	11.4000	8.82	10.1398	42.6153	2.742	-4.0508
11	-110.368	11.4000	8.82	11.5884	54.2433	2.742	-21.5743
12	-120.000	10.3740	8.82	11.5884	58.1400	2.742	-28.3356
13	-45.000	9.7750	8.82	13.0370	54.0702	2.742	43.4446
14	-120.000	10.6305	8.82	13.7612	46.5120	2.742	-37.5343
15	-49.200	11.4000	8.82	14.4855	34.8840	2.742	23.1315
16	-33.7994	11.4000	8.82	13.7612	27.1527	2.742	30.0765
17	-3.4848	11.4000	8.82	12.6700	11.6280	2.742	43.7752
18	-0.2431	11.4000	8.82	11.5884	7.7339	2.742	42.0412
19	10.5000	2.3655	8.82	9.4156	0	2.742	33.8431
20	2.6768	11.4000	8.82	6.5185	0	2.742	32.1572
21	-1.7983	11.4000	8.82	6.1558	0	2.742	27.3195
22	-3.8810	11.4000	8.82	4.7072	0	2.742	23.7883
23	9.0000	-4.2609	8.82	3.9840	0	2.742	20.2851
24	7.8000	-7.0824	8.82	3.2598	0	2.742	15.5393

Table 5. Comparison of RO and DRCC methods.

Method	RO	DRCC
MG operation cost (€ct)	527.3476	416.1213

electricity price hours, excess power is sold to the grid, generating profit. During hours when the grid price is lower than the cost of using the MG's power generation resources, the required power is drawn from the main grid to minimize costs. The QTLBO is compared with TLBO, DE, and RCGA. The operational costs resulting from the QTLBO, TLBO, DE, and RCGA algorithms are 416.1213 €ct, 428.9162 €ct, 446.2825 €ct, and 453.2905 €ct, respectively. Simulation results demonstrate the effectiveness of the QTLBO algorithm in achieving an optimal solution and show faster convergence to the final solution compared to TLBO, DE, and RCGA. Additionally, the results are compared with those obtained from uncertainty modeling using the RO method. The findings indicate that the DRCC method achieves a 23.58% lower operating cost than the RO method.

In future work, we will conduct a comprehensive quantitative comparison of the DRCC and RO methods by evaluating their economic recovery, risk profiles, and associated trade-offs. We will also perform extensive sensitivity analyses on key model parameters such as resource capacities, market prices, and confidence levels, including a dedicated assessment of how the DRCC confidence level affects operational cost and solution robustness. Furthermore, we will simulate multiple operational scenarios under varied PV/WT penetration rates, uncertainty levels, and market conditions, and extend the comparative analysis to include more recent and state-of-the-art algorithms beyond classical approaches. Additionally, we will examine the computational burden and complexity introduced by DRCC constraints and compare these results with CCP and RO formulations. Finally, we will provide a detailed evaluation of resource utilization patterns—including PV, WT, FC, and MT—and analyze their interactions and effects on operational costs and network stability.

ACKNOWLEDGEMENT

The authors declare that no artificial intelligence tools were used in the preparation, writing, or revision of this manuscript.

REFERENCES

[1] M. Rodriguez, D. Arcos-Aviles, and W. Martinez, "Fuzzy logic-based energy management for isolated microgrid using meta-heuristic optimization algorithms," *Appl. Energy*, vol. 335, p. 120771, 2023.

[2] M. H. Alabdullah and M. A. Abido, "Microgrid energy management using deep Q-network reinforcement learning," *Alexandria Eng. J.*, vol. 61, no. 11, pp. 9069–9078, 2022.

[3] M. N. Alam, S. Chakrabarti, and A. Ghosh, "Networked microgrids: State-of-the-art and future perspectives," *IEEE Trans. Ind. Informat.*, vol. 15, no. 3, pp. 1238–1250, 2018.

[4] E. Shahrabi, S. M. Hakimi, A. Hasankhani, G. Derakhshan, and B. Abdi, "Developing optimal energy management of energy hub in the presence of stochastic renewable energy resources," *Sustain. Energy Grids Netw.*, vol. 26, p. 100428, 2021.

[5] M. Daneshvar, B. Mohammadi-Ivatloo, M. Abapour, S. Asadi, and R. Khanjani, "Distributionally robust chance-constrained transactive energy framework for coupled electrical and gas microgrids," *IEEE Trans. Ind. Electron.*, vol. 68, no. 1, pp. 347–357, 2020.

[6] Y. Zhou, W. Yu, S. Zhu, B. Yang, and J. He, "Distributionally robust chance-constrained energy management of an integrated retailer in the multi-energy market," *Appl. Energy*, vol. 286, p. 116516, 2021.

[7] R. Rashidi, A. Hatami, M. Moradi, and X. Liang, "Optimal multi-microgrids energy management through information gap decision theory and tunicate swarm algorithm," *IEEE Access*, 2024.

[8] X. Fan, Y. Chen, R. Wang, J. Luo, J. Wang, and D. Cao, "Integrated energy microgrid economic dispatch optimization

model based on information-gap decision theory," *Energies*, vol. 16, no. 8, p. 3314, 2023.

[9] S. Rong *et al.*, "Information gap decision theory-based stochastic optimization for smart microgrids with multiple transformers," *Appl. Sci.*, vol. 13, no. 16, p. 9305, 2023.

[10] Y. Zou, Y. Xu, and C. Zhang, "A risk-averse adaptive stochastic optimization method for transactive energy management of a multi-energy microgrid," *IEEE Trans. Sustain. Energy*, vol. 14, no. 3, pp. 1599–1611, 2023.

[11] H. Abunima, W.-H. Park, M. B. Glick, and Y.-S. Kim, "Two-stage stochastic optimization for operating a renewable-based microgrid," *Appl. Energy*, vol. 325, p. 119848, 2022.

[12] M. S. AlDavood, A. Mehbodniya, J. L. Webber, M. Ensaf, and M. Azimian, "Robust optimization-based optimal operation of islanded microgrid considering demand response," *Sustainability*, vol. 14, no. 21, p. 14194, 2022.

[13] P. K. Mianaei, M. Aliahmadi, S. Faghri, M. Ensaf, A. Ghasemi, and A. A. Abdoos, "Chance-constrained programming for optimal scheduling of combined cooling, heating, and power-based microgrid coupled with flexible technologies," *Sustain. Cities Soc.*, vol. 77, p. 103502, 2022.

[14] K. A. A. Sumarmad, N. Sulaiman, N. I. A. Wahab, and H. Hizam, "Microgrid energy management system based on fuzzy logic and monitoring platform for data analysis," *Energies*, vol. 15, no. 11, p. 4125, 2022.

[15] S. Wang, Q. Tan, X. Ding, and J. Li, "Efficient microgrid energy management with neural-fuzzy optimization," *Int. J. Hydrogen Energy*, vol. 64, pp. 269–281, 2024.

[16] L. P. Raghav, R. S. Kumar, D. K. Raju, and A. R. Singh, "Optimal energy management of microgrids using quantum teaching learning based algorithm," *IEEE Trans. Smart Grid*, vol. 12, no. 6, pp. 4834–4842, 2021.

[17] M. Hojjat and A. Ghasemi, "A chance-constrained programming approach to solve the energy management problem in microgrids considering uncertainties of renewable energy resources," in *Proc. Int. Conf. Electr., Comput. Energy Technol.*, pp. 1–7, IEEE, 2024.

[18] M. Mohiti, M. Mazidi, N. Oggioni, D. Steen, and L. A. Tuan, "An IGDT-based energy management system for local energy communities considering phase-change thermal energy storage," *IEEE Trans. Ind. Appl.*, vol. 60, no. 3, pp. 4470–4481, 2024.

[19] Z. Esmaeili and S. H. Hosseini, "Optimal energy management of microgrids using quantum teaching learning based algorithm," *AUT J. Electr. Eng.*, vol. 55, no. 2, pp. 225–240, 2023.

[20] C. Duan, W. Fang, L. Jiang, L. Yao, and J. Liu, "Distributionally robust chance-constrained approximate AC-OPF with Wasserstein metric," *IEEE Trans. Power Syst.*, vol. 33, no. 5, pp. 4924–4936, 2018.

[21] H. Qiu, W. Gu, Y. Xu, and B. Zhao, "Multi-time-scale rolling optimal dispatch for AC/DC hybrid microgrids with day-ahead distributionally robust scheduling," *IEEE Trans. Sustain. Energy*, vol. 10, no. 4, pp. 1653–1663, 2018.

[22] M. Mahmoudi, B. Alizadeh, and S. Dehghan, "Distributionally robust chance-constrained transmission expansion planning using a distributed solution," *IEEE Trans. Netw. Sci. Eng.*, 2024.

[23] M. Rayati, M. Bozorg, R. Cherkaoui, and M. Carpita, "Distributionally robust chance constrained optimization for providing flexibility in an active distribution network," *IEEE Trans. Smart Grid*, vol. 13, no. 4, pp. 2920–2934, 2022.

[24] M. Dashtdar, M. Bajaj, and S. M. S. Hosseinimoghadam, "Design of optimal energy management system in a residential microgrid based on smart control," *Smart Sci.*, vol. 10, no. 1, pp. 25–39, 2022.

[25] O. H. M. J. I. A. Ross, "A review of quantum-inspired metaheuristics: Going from classical computers to real quantum computers," *IEEE Access*, vol. 8, pp. 814–838, 2019.

[26] Y. Li, M. Tian, G. Liu, C. Peng, and L. Jiao, "Quantum optimization and quantum learning: A survey," *IEEE Access*, vol. 8, pp. 23568–23593, 2020.

[27] Z. Shi, H. Liang, S. Huang, and V. Dinavahi, "Distributionally robust chance-constrained energy management for islanded microgrids," *IEEE Trans. Smart Grid*, vol. 10, no. 2, pp. 2234–2244, 2018.

[28] D. Huo, C. Gu, K. Ma, W. Wei, Y. Xiang, and S. Le Blond, "Chance-constrained optimization for multienergy hub systems in a smart city," *IEEE Trans. Ind. Electron.*, vol. 66, no. 2, pp. 1402–1412, 2018.

[29] F. Zou, D. Chen, and Q. Xu, "A survey of teaching–learning-based optimization," *Neurocomputing*, vol. 335, pp. 366–383, 2019.

[30] A. Kaveh, M. Kamalinejad, K. B. Hamedani, and H. Arzani, "Quantum teaching-learning-based optimization algorithm for sizing optimization of skeletal structures with discrete variables," in *Structures*, vol. 32, pp. 1798–1819, Elsevier, 2021.

[31] A. A. Moghaddam, A. Seifi, T. Niknam, and M. R. A. Pahlavani, "Multi-objective operation management of a renewable microgrid with back-up micro-turbine/fuel cell/battery hybrid power source," *Energy*, vol. 36, no. 11, pp. 6490–6507, 2011.